An Open-Loop Control for Underactuated Manipulators Using Oscillatory Inputs: Steering Capability of an Unactuated Joint

Keum-Shik Hong

***Abstract*—An open-loop control for underactuated mechanical systems using oscillatory inputs with amplitude and frequency modulations is investigated. Once all actuated joints are moved to their desired positions, oscillatory inputs are applied to an actuated joint to move the remaining unactuated joints. The steering force of the unactuated joints is achieved by utilizing the dynamic coupling between actuated and unactuated joints. Such a dynamic coupling occurs due to the oscillatory motions of an actuated joint. Once the frequency of the oscillatory input is decided, the amplitude is determined by analyzing a time-invariant system, which is derived from the unactuated joint dynamics by the method of averaging. A systematic way, via a generating equation and a coordinate transformation derived from the generating equation, for converting the unactuated joint dynamics into the standard form of averaging is proposed. In the event of an actuator failure in outer space, the failed joint can be steered by adopting the method proposed. Illustrating examples are given. Experimental results are provided.**

***Index Terms*—Asymptotic method, averaging, open-loop control, underactuated manipulator, vibrational control.**

I. Introduction

An underactuated mechanical system refers to a system with less number of actuators than the degree-of-freedom of the system considered. Therefore, manipulators with passive or free joints are underactuated systems because the number of control inputs is smaller than the number of generalized coordinates. Recent focuses in the area of underactuated systems control are a reduction of the number of actuators and/or sensors and an improvement of the reliability through a fault-tolerant design of fully actuated manipulators that are working in hazardous areas or with dangerous materials. It is particularly important for a space robot working in outer space to have the ability to control the failed joint in the event of an actuator failure.

An active (or actuated) joint is one that is fully controlled with an actuator, while a passive joint is one which has no actuation but is equipped with a passive element like a damper or a brake. A free joint is one that can move freely. Underactuated systems are defined as those with passive and/or free joints.

Control of the unactuated parts of underactuated mechanical systems is, in general, achieved by utilizing either kinematic or dynamic couplings [1]–[3], [9], [12], [18], [20]–[23], [28]–[31]. Examples utilizing kinematic coupling are first-order nonholonomic systems such as wheeled mobile robots and dexterous robot hands. The equations of these systems are drift-free with inputs entering linearly. The second class of systems characterized by dynamic coupling is provided by numerous examples; a crane system, the classical cart-pole system, an acrobot, and manipulators with flexible elements. The equations of the second class involve a drift term accounting for gravitational, centripetal, Coriolis, and/or elastic forces with inputs entering affinely. The class of underactuated systems considered in this paper belongs to the second class. It is also noted that underactuation does not always imply uncontrollability. The controllability depends on the structure of the system considered. All previous examples are controllable. However, in the case of a planar manipulator with a free joint [12], [21], [29]–[31], the linearized equation at any operating point is not controllable.

Several researchers have investigated underactuated systems with passive joints. Arai and Tachi [1] proved that the number of active joints must be equal to or greater than the number of passive ones in order to control the passive ones. A Cartesian space controller to bring all the joints to their desired set points was also developed [2]. Saito *et al.* [22] developed a two link underactuated brachiating robot which is capable of moving along crossbars using only one actuator. Bergerman and Xu [9] investigated a variable structure control for a three-link manipulator with one passive joint in both joint and Cartesian spaces.

Compared with the works for the systems with passive joints, controls of the systems with free joints are very rare. Spong [28] investigated the swing up control problem for the acrobot using partial feedback linearization and energy-based method. Recently, a scholastic work by Nakamura *et al.* [21], see also [29]–[31], investigated the application of periodic oscillations to control the manipulators with free joints. An oscillatory control based on Poincare map analysis has also appeared in [30]. De Luca *et al.* [18] have proposed a constructive open-loop control strategy that involves nilpotent approximation and iterative steps.

Comparing the work of this paper and the work of Suzuki and Nakamura [29]–[31], the tools used for analysis are the same, i.e., partial feedback linearization technique and averaging method [3]–[8], [10], [13]–[17], [19], [24], [25] are used. Also, a planar 2R manipulator is taken as an illustrating example. But, important differences are: In this paper, a systematic design method of input amplitudes and frequencies is proposed. The utilization of a generating equation and a coordinate transformation, which converts the equations of unactuated joints dynamics into the standard form of averaging, is suggested. How the generating equation can be deduced from the equations of unactuated joints dynamics is also explained. A step-by-step design procedure of control inputs is demonstrated using a planar manipulator with a passive joint as well as a free joint. In Suzuki

Manuscript received November 30, 2000; revised September 27, 2001. Manuscript received in final form November 20, 2001. Recommended by Associate Editor S. S. Ge. This work was supported by the Korea Research Foundation under Grant KRF 2001-041-E00075.

The author is with the School of Mechanical Engineering, Pusan National University, Pusan 609-735, Korea (e-mail: kshong@pusan.ac.kr).

Publisher Item Identifier S 1063-6536(02)01767-0.

and Nakamura [29], the averaged system of the 2R manipulator involves the input frequency. However, in this work, the averaged system involves input amplitude and is free of input frequency. Also, the reciprocal of the input frequency appears in front of the averaged equation. Hence the closeness of the averaged system and the original system is assured by increasing the input frequency.

Under the name of vibrational control, an open-loop control technique utilizing parametric excitations with amplitude modulation has been extensively investigated [4]–[8], [14]–[17], [19]. Note that the active joint variables appearing in an unactuated joint's dynamics can be considered as time-varying parameters. Therefore, a periodic motion of an active joint acts as a parametric vibrational control for controlling the unactuated joint. In vibrational control, the averaging theory plays a key roll in determining the stability properties. As far as controlling a planar manipulator with a free joint is concerned, the input shaping method [26] is not applicable. Every linearized plant is not controllable by the definition of controllability for linear systems. Furthermore, the notion of natural frequency is not available since the second free joint is moving in the horizontal plane. No conventional control methods including the input shaping method can be applied to this system.

In this paper the steering problem of an unactuated joint via a parametric vibrational control is investigated. The control procedure consists of two stages. The first stage linearizes the system partially, and applies a proper control technique to drive the active joints to their desired locations. At the end of first stage, the positions of unactuated joints will be arbitrary. Then, periodic vibrations are introduced to an actuated joint to move the unactuated joint to its target position. The magnitudes of the oscillatory inputs are determined from an averaged system.

The contributions of this paper are as follows. This paper discusses a novel open-loop control technique that provides a viable tool when the conventional control schemes are not applicable and/or actuator failure occurs. Averaging analysis is extended to the systems with the derivatives and antiderivatives of vibrations. And, a systematic method of obtaining a generating equation and a coordinate transformation that lead to an averaged system of unactuated joint dynamics is developed. A manipulator in outer space with a failed joint can be controlled in this fashion.

II. Vibrational Control of an Underactuated System

The class of underactuated systems focused in this paper is such systems that the conventional control methods are not readily applicable. Examples of this class include a planar manipulator with a free joint, a two-link manipulator of which the actuated link is in the horizontal direction but the unactuated link is in the vertical direction, etc. Particularly, a manipulator in outer space with a failed joint belongs to this class, because there is no gravity in outer space. Since vibrational control is an open-loop control method, a precise mathematical model of the system is needed.

A. Partially Linearized Form

The steering force for an unactuated joint is invoked by applying periodic vibrations to its adjacent actuated joint. To see that the oscillatory inputs applied to an actuated joint causes the dynamic coupling (the steering force), a partially linearized form of the system is derived.

Consider a k degree-of-freedom manipulator with $q_1 \in R^m$ actuated joints and $q_2 \in R^l$ unactuated joints, where $l = k-m$, as follows:

$$M_{11}(q)\ddot{q}_1 + M_{12}(q)\ddot{q}_2 + C_1(q,\dot{q}) + G_1(q) = \tau \quad (1)$$

$$M_{21}(q)\ddot{q}_1 + M_{22}(q)\ddot{q}_2 + C_2(q,\dot{q}) + G_2(q) = 0. \quad (2)$$

The vector functions $C_1(q,\dot{q}) \in R^m$ and $C_2(q,\dot{q}) \in R^l$ contain Coriolis and centripetal terms, the vector functions $G_1(q) \in R^m$ and $G_2(q) \in R^l$ contain gravitational terms, and $\tau \in R^m$ represents the input generalized force produced by m actuators at the active joints. It is assumed that each joint has a single degree of freedom and all joint variables are measured. A feedback linearizing control law [28] is introduced as follows:

$$\tau = \left(M_{11} - M_{12}M_{22}^{-1}M_{21}\right)u + \left(C_1 - M_{12}M_{22}^{-1}C_2\right) + \left(G_1 - M_{12}M_{22}^{-1}G_2\right)$$

where $u \in R^m$ is an additional control input to be yet specified. The substitution of τ into (1) yields a partially linearized system as follows:

$$\ddot{q}_1 = u, \quad (3)$$

$$M_{22}(q)\ddot{q}_2 + C_2(q,\dot{q}) + G_2(q) = -M_{21}(q)u. \quad (4)$$

Observing (4), it is clear that q_1-terms behave as parameters in q_2-dynamics. Therefore, if an oscillatory input to an actuated joint is applied, its motion becomes time-varying parameters in the equations of unactuated joints.

It is now assumed that all actuated joints have reached their set points with an appropriate control input, i.e., $u = \ddot{q}_{1d} - \Lambda_1(\dot{q}_1 - \dot{q}_{1d}) - \Lambda_2(q_1 - q_{1d})$ would suffice this goal, where Λ_1 and Λ_2 are design parameters. During this transition, the positions of unactuated joints will be governed by the dynamics of (4).

B. Selection of a Vibratile Parameter

With an oscillatory motion of q_1, the unactuated joint dynamics can be written as

$$M_{22}(q_2;q_1)\ddot{q}_2 + C_2\left(q_2,\dot{q}_2;q_1,\dot{q}_1\right) + G_2(q_2;q_1) + M_{21}(q_2;q_1)\ddot{q}_1 = 0 \quad (5)$$

where q_1, $\dot{q}_1$, and $\ddot{q}_1$ are time-varying parameters in (5). It is also remarked that because the input is periodic and the amplitude of the vibration is very small, the original set point of the actuated joint can be kept within a specified error bound.

Define the state vector of (5) as $x = \begin{bmatrix} q_2 & \dot{q}_2 \end{bmatrix}^T \in R^n$, where $n = 2l$. Then, the state equation becomes (6a)–(c) shown at the bottom of the next page, where $X: R^n \rightarrow R^n$. q_1, $\dot{q}_1$, and $\ddot{q}_1$ are now considered as system parameters in (6b). In (6c), the symbol λ is introduced to emphasize the fact that there exists one selective parameter in which vibrations can be introduced. It is also remarked that only a subset of $\{q_1, \dot{q}_1, \ddot{q}_1\}$ may appear

in (6a) depending on the structure of the underactuated systems considered.

In this paper, λ is taken as the second highest derivative in the set $\{q_1, \dot{q}_1, \ddot{q}_1\}$. For example, if only q_1 and $\dot{q}_1$ appear in (6a), then $\lambda = q_1$. By choosing the second highest derivative as a vibratile parameter, the existence of a coordinate transformation that will transform (6a) into the standard form of averaging is guaranteed.

Assuming that all q_1, $\dot{q}_1$, and $\ddot{q}_1$ appear in (6a), i.e., $\lambda(t) = \dot{q}_1(t)$, an oscillatory input is introduced into (6c) as follows:

$$\lambda(t) \to \lambda_0 + \alpha f(\omega t) \tag{7}$$

where λ_0 is a constant and $\alpha f(\omega t)$ is a zero mean T-periodic function in which α and ω denote its amplitude and frequency. The following relations also hold:

$$\ddot{q}_1 = \alpha\omega f'(\omega t) \tag{8}$$

and

$$q_1 = \frac{\alpha}{\omega} F(\omega t) + \lambda_0 t + q_{1d} \tag{9}$$

where f' and F are the derivative and the anti-derivative of f, respectively, and q_{1d} is the desired position of q_1. The substitution of (7)–(9) into (6) yields

$$\begin{aligned}\dot{x} =& X(x; \lambda_0 + \alpha f(\omega t)) \\ =& \begin{bmatrix} x_2 \\ -M_{22}^{-1}\left(x_1, \frac{\alpha}{\omega}F(\omega t) + \lambda_0 t + q_{1d}\right) \\ \times \Big\{ C_2\left(x_1, x_2, \frac{\alpha}{\omega}F(\omega) + \lambda_0 t + q_{1d}, \lambda_0 + \alpha f(\omega t)\right) \\ + G_2\left(x_1, \frac{\alpha}{\omega}F(\omega t) + \lambda_0 t + q_{1d}\right) \\ + \alpha\omega M_{21}\left(x_1, \frac{\alpha}{\omega}F(\omega t) + \lambda_0 t + q_{1d}\right) f'(\omega t) \Big\} \end{bmatrix}. \end{aligned} \tag{10}$$

Note that (10) is a time-varying system. For the given control task, designing α and ω by analyzing (10) is not simple. This is the reason why the asymptotic method of averaging is utilized in the sequel. It will be shown that there exists a lower frequency bound ω_0 such that for all $\omega \geq \omega_0$, the stability properties of (10) and those of a time-invariant system associated with (10) are the same. Therefore, the determination of α and ω in (7) is based upon the dynamics of an averaged time-invariant system representing (10).

C. Transformation and the Standard Form of Averaging

Assume that (10) is decomposed into two parts as follows:

$$\dot{x} = X_0\left(x, \omega t, \frac{1}{\omega}\right) + \omega X_1(x, \omega t). \tag{11}$$

The second term of (11) is a collection, or a partial collection, of the terms that are multiplied by ω. The decomposition in (11) is always possible because the second highest derivative among q_1, $\dot{q}_1$, and $\ddot{q}_1$ in (6b) has been chosen as the vibratile parameter and therefore the highest derivative yields ω when it is differentiated.

The second term of (11) is now used as a tool for generating a coordinate transformation that will transform (10) into the standard form of averaging. Therefore, an equation for generating a coordinate transformation (in short, a generating equation) takes the form as

$$\dot{\xi}(t) = X_1(\xi, t), \quad \xi(0) = c \tag{12}$$

where ξ denotes the state vector of the generating equation and $c \in R^n$ is the initial condition. Let $h(t, c)$: $R \times R^n \to R^n$ be the general solution of (12). The specification of the initial condition is not needed in this work, because only the form of $h(t, c)$ is used as a coordinate transformation. Note that $h(t, c)$ should be T-periodic because X_1 is T-periodic.

Now, introducing a new variable $p(t)$, a coordinate transformation is defined as follows:

$$x(t) = h(\omega t, p(t)). \tag{13}$$

Note that t and c in $h(t, c)$ have been replaced by ωt and $p(t)$, respectively. Therefore, the differentiation of both sides of (13) with respect to t yields

$$\dot{x} = \frac{\partial h}{\partial p}\frac{\partial p}{\partial t} + \frac{\partial h}{\partial \omega t}\frac{\partial \omega t}{\partial t} = \frac{\partial h}{\partial p}\dot{p} + \omega\frac{\partial h}{\partial \omega t}. \tag{14}$$

Comparing (11) and (14) and noting that h is the solution of (12), (14) yields

$$\dot{p}(t) = \left[\frac{\partial h(\omega t, p(t))}{\partial p}\right]^{-1} X_0\left(h(\omega t, p(t)), \omega t, \frac{1}{\omega}\right). \tag{15}$$

To investigate the dynamics of (15) in a slow time scale, another new state vector such that $z(\tau) = p(\tau)$, $\tau = \omega t$, where τ denotes a slow time scale, is introduced. Then, the following holds:

$$\dot{p}(t) = \frac{dz(\omega t)}{d\omega t}\frac{d\omega t}{dt} = \omega z'$$

where $z' = dz(\tau)/d\tau$. Therefore, by substituting $\dot{p} = \omega z'$, $z(\tau) = p(t)$, $\tau = \omega t$, and $\varepsilon \triangleq 1/\omega$ into (15), the standard form of averaging [10], [13], and [24] is derived as follows:

$$z'(\tau) = \varepsilon\left[\frac{\partial h(\tau, z(\tau))}{\partial z}\right]^{-1} X_0\left(h(\tau, z(\tau)), \tau, \varepsilon\right). \tag{16}$$

$$\dot{x} = \begin{bmatrix} x_2 \\ -M_{22}^{-1}(x_1, q_1)\left\{C_2(x_1, x_2, q_1, \dot{q}_1) + G_2(x_1, q_1) + M_{21}(x_1, q_1)\ddot{q}_1\right\} \end{bmatrix} \tag{6a}$$

$$\triangleq X(x; q_1, \dot{q}_1, \ddot{q}_1) \tag{6b}$$

$$\triangleq X(x; \lambda) \tag{6c}$$

D. Averaging Analysis

Consider the following differential equation in the standard form of averaging:

$$\dot{z}(t) = \varepsilon g(z(t), t, \varepsilon), \quad z(0) = z_0 \tag{17}$$

where $z \in R^n$, $t \geq 0$, $0 < \varepsilon \leq \varepsilon_0$, and g is piecewise continuous in t. Note that for a small ε, the time-variation of z is slow as compared to the time-variation of g. The existence of ε_0 is also assured in our case because ε was defined by $1/\omega$. The existence of the standard form of averaging for an underactuated manipulator is stated as follows.

Theorem 1: Consider the underactuated system (1) and (2). Then there exist a parametric vibration and a coordinate transformation with which the dynamics of unactuated joints can be represented in the standard form of averaging as (17).

Proof: All developments above are already self-explanatory. Since the actuated joint variables are treated as vibratile parameters in unactuated dynamics (6a), it is always possible to introduce vibrations like (7). Among the three variables $\{q_1, \dot{q}_1, \ddot{q}_1\}$ that would possibly appear in the right-hand side of (6a), the second highest term has been selected as a vibratile parameter. This allows the existence of X_1-term in (11). The existence of a coordinate transformation that converts system (11) into the standard form of averaging is evident from the existence of a generating equation (12). Finally, system (16) is the desired form. □

Theorem 1 opens only the possibility of vibrational control for an underactuated system. It does not say yet whether the vibrations would stabilize the system or steer an unactuated joint, etc. It is also not obvious yet which joint has to be vibrated or how many joints need to be vibrated. These questions can be answered only when (16) is fully analyzed. Because the averaging method allows us to investigate the stability properties of (17) via a time-invariant system derived from (17), the averaging procedure for (17) is performed as follows.

The mean value of $g(z, t, \varepsilon)$ is defined as follows:

$$g_{\text{av}}(z) \triangleq \lim_{T \to \infty} \frac{1}{T} \int_{t_0}^{t_0+T} g(z, \sigma, 0) d\sigma. \tag{18}$$

It is assumed that the limit in (18) exists uniformly in t_0 and z. Then, the averaged system associated with (17) is defined as

$$\dot{y}(t) = \varepsilon g_{\text{av}}(y(t)), \quad y(0) = z_0 \tag{19}$$

where y denotes the state vector of the averaged system. The following results are readily available in the literature.

Basic Averaging Theorem (See [25, p. 172]): Let systems (17) and (19) satisfy the following assumptions: 1) $z = 0$ is an equilibrium point of system (17); 2) $g(z, t, \varepsilon)$ is locally Lipschitz continuous in both x and ε; 3) $y = 0$ is an equilibrium point of system (19); 4) $g_{\text{av}}(y)$ is locally Lipschitz continuous in y; and 5) $e(z, t) \equiv g(z, t, 0) - g_{\text{av}}(z)$ is piecewise continuous in t, has bounded and continuous partial derivatives in z, and $e(0, t) = 0$, for all $t \geq 0$. Moreover, $e(z, t)$ and $\partial e(z, t)/\partial z$ have zero mean values. Then, there exists a continuous and strictly increasing function $\varphi(\varepsilon)$ with $\varphi(0) = 0$ such that for a given $T \geq 0$

$$\|z(t) - y(t)\| \leq \varphi(\varepsilon) b_T$$

for some $b_T \geq 0$, $\varepsilon_0 > 0$ and for all $t \in [0, T/\varepsilon]$ and $\varepsilon \leq \varepsilon_0$.

Remark 1: The basic averaging theorem establishes the closeness of the two trajectories of (17) and (19) on the time interval $[0, T/\varepsilon]$, where ε is arbitrarily small. The error is in the order of $\varphi(\varepsilon)$ which can be made arbitrarily small by decreasing ε. Although the interval $[0, T/\varepsilon]$ is unbounded as $\varepsilon \to 0$, the result does not allow us to compare the stability properties of the two systems yet.

Exponential Stability Theorem (See [25, p. 173]): Let systems (17) and (19) satisfy assumptions 1)–5) of the basic averaging theorem. Assume further that system (19) satisfies 6) $g_{\text{av}}(y)$ has continuous and bounded first partial derivatives in y and 7) $y = 0$ is an exponentially stable equilibrium point. Then, $z = 0$ of (17) is exponentially stable for ε sufficiently small.

Remark 2: The exponential stability theorem states how a local exponential stability result for (17) can be deduced from (19). It is also noted that the global exponential stability can be stated if the averaged system is globally exponentially stable and if all assumptions are valid globally.

Remark 3: The existences of an upper bound, ε_0, in the basic averaging theorem and a sufficiently small ε in the exponential stability theorem are all guaranteed in our case, because ε was defined by $1/\omega$. By increasing ω, the frequency of vibration, the closeness of the two solutions or the stability properties of the two systems are assured once ω passes over the critical frequency. The question such that how small ε should be, or how large ω should be, can be reasonably answered by computer simulations. This is because analytic methods sometimes give very conservative results that are not meaningful for real applications. In Section III-B, a lower bound ω_0 for a 2R manipulator is estimated.

Remark 4: The method in this paper illustrates one systematic way of obtaining an averaged system. It is noted that the coordinate transformations and averaged systems are not unique. However, obtaining a meaningful averaged system that provides stability results for the original system is important. Even though a general procedure for vibrational control for an underactuated mechanical system has been described in Section II, the questions like what joint has to be vibrated or how many joints need to be vibrated are problem-dependent.

III. Examples of Control Law Design

In this section, to illustrate control system design for underactuated mechanical systems, the procedure of Section II is applied to a planar 2R manipulator. As shown in the sequel, this method can steer a passive joint as well as a free joint to their target positions. Note that the linear control methods are not applicable to these examples, because the linearized system of a planar 2R manipulator is not controllable. Note also that if one actuator of a manipulator in outer space fails, then all masses of the links before and after the failed joint can be combined into two equivalent masses. Therefore, the problem can be reduced to the problem of controlling a two-link manipulator.

A. A Planar Manipulator With a Free Joint

Fig. 1(a) shows a schematic diagram of the planar manipulator in which the second joint is free. Fig. 1(b) shows an exper-

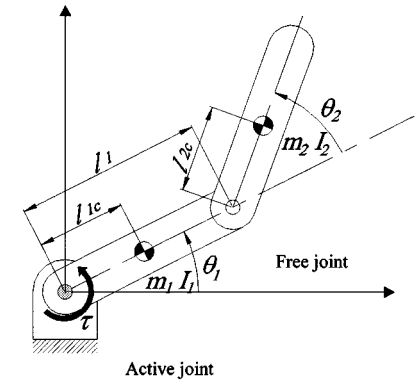

(a)

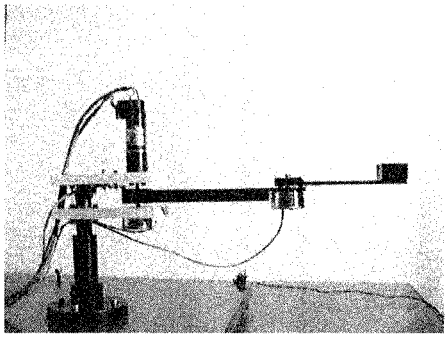

Parameters	link 1	link 2
mass(10^{-3} kg)	200	255
Inertia(10^{-3} kgm^2)	3.097	3.499
Length(10^{-3} m)	185	135
Distance to mass center (10^{-3} m)	103	60

(b)

Fig. 1. A planar 2R manipulator with an unactuated joint. (a) Schematic diagram of a planar 2R manipulator. (b) An experimental 2R manipulator setup and its parameters.

imental manipulator together with parameter values tabulated below. Using the Lagrange equation, the following equations of motion are obtained:

$$\begin{aligned} M_{11}(\theta_2)\ddot{\theta}_1 + M_{12}(\theta_2)\ddot{\theta}_2 + C_1\left(\theta_2, \dot{\theta}_1, \dot{\theta}_2\right) &= \tau, \\ M_{12}(\theta_2)\ddot{\theta}_1 + M_{22}(\theta_2)\ddot{\theta}_2 + C_2\left(\theta_2, \dot{\theta}_1, \dot{\theta}_2\right) &= 0 \end{aligned} \tag{20}$$

where

$$\begin{aligned} M_{11}(\theta_2) &= m_1 l_{1c}^2 + m_2 l_1^2 + m_2 l_{2c}^2 + 2m_2 l_{2c} l_1 \cos\theta_2 \\ &\quad + I_1 + I_2, \\ M_{12}(\theta_2) &= m_2 l_{2c}^2 + m_2 l_{2c} l_1 \cos\theta_2 + I_2 \\ M_{22}(\theta_2) &= m_2 l_{2c}^2 + I_2 \\ C_1\left(\theta_2, \dot{\theta}_1, \dot{\theta}_2\right) &= -m_2 l_{2c} l_1 \sin\theta_2 \left(2\dot{\theta}_1\dot{\theta}_2 + \dot{\theta}_2^2\right) \\ C_2\left(\theta_2, \dot{\theta}_1, \dot{\theta}_2\right) &= 2m_2 l_{2c} l_1 \dot{\theta}_1^2 \sin\theta_2. \end{aligned}$$

Note that the gravity term does not appear in the equations, and check that the linearized equation at an operating point $\left(\theta_1, \theta_2, \dot{\theta}_1, \dot{\theta}_2\right) = (\theta_1, \theta_2, 0, 0)$ is not controllable.

Following the procedure of Section II-A, a partially linearized system, (3) and (4), is derived as follows:

$$\ddot{\theta}_1 = u \tag{21a}$$

$$\ddot{\theta}_2 = -(1 + d\cos\theta_2)\ddot{\theta}_1 - d\dot{\theta}_1^2 \sin\theta_2 \tag{21b}$$

where $d = m_2 l_1 l_{2c} / \left(m_2 l_{2c}^2 + I_2\right)$ is a constant. Now, assume that the active joint θ_1 has been positioned at its desired location with an appropriate control action. For instance

$$u = \ddot{\theta}_{1d} + k_v\left(\dot{\theta}_{1d} - \dot{\theta}_1\right) + k_p(\theta_{1d} - \theta_1)$$

would suffice, in which k_p and k_v are position and velocity gains. While the active joint moves to its target position, the position of the free joint will be governed by (21b). Now, the control task is restricted to controlling the free joint. With the state variables defined by $x_1 = \theta_2$ and $x_2 = \dot{\theta}_2$, the state equation of (21b) becomes

$$\begin{aligned} \dot{x}_1 &= x_2, \quad x_1(0) = x_{10} \\ \dot{x}_2 &= -(1 + d\cos x_1)\ddot{\theta}_1 - d\sin x_1 \left(\dot{\theta}_1\right)^2, \; x_2(0) = x_{20}. \end{aligned} \tag{22}$$

Note that (22) corresponds to (6a). Observing that $\dot{\theta}_1$ is the second highest derivative appearing in (22), introduce vibrations according to law (7) as follows:

$$\lambda(t) = \dot{\theta}_1(t) \to 0 + \alpha\sin\omega t. \tag{23}$$

Hence, $\lambda_0 = 0$ and $\alpha f(\omega t) = \alpha\sin\omega t$ have been selected. The following also holds:

$$\theta_1(t) = -\frac{\alpha}{\omega}\cos\omega t + \theta_{1d} \tag{24}$$

and

$$\ddot{\theta}_1(t) = \alpha\omega\cos\omega t. \tag{25}$$

Equation (24) implies that once α and ω are determined, the first joint must oscillate with amplitude α/ω and frequency ω. Hence, by increasing ω, the amplitude of vibrations will get smaller. The substitution of (23)–(25) into (22) yields

$$\begin{aligned} \begin{bmatrix} \dot{x}_1 \\ \dot{x}_2 \end{bmatrix} &= \begin{bmatrix} x_2 \\ -d\alpha^2 \sin x_1 \sin^2\omega t \end{bmatrix} \\ &\quad + \omega \begin{bmatrix} 0 \\ -\alpha\cos\omega t(1 + d\cos x_1) \end{bmatrix} \\ &\triangleq X_0\left(x, \omega t, \frac{1}{\omega}\right) + \omega X_1(x, \omega t). \end{aligned} \tag{26}$$

Note that (26) is in the form of (11). Therefore, the generating equation of (12) takes the form

$$\begin{bmatrix} \dot{\xi}_1 \\ \dot{\xi}_2 \end{bmatrix} = \begin{bmatrix} 0 \\ -\alpha\cos t(1 + d\cos\xi_1) \end{bmatrix}, \quad \xi(0) = \begin{bmatrix} c_1 \\ c_2 \end{bmatrix}. \tag{27}$$

The general solution of (27) is given by

$$h(t, c) = \begin{bmatrix} h_1(t, c) \\ h_2(t, c) \end{bmatrix} = \begin{bmatrix} c_1 \\ c_2 - \alpha(1 + d\cos c_1)\sin t \end{bmatrix}. \tag{28}$$

A coordinate transformation that will convert (26) into the standard form of averaging is defined using (28) as

$$\begin{bmatrix} x_1(t) \\ x_2(t) \end{bmatrix} = \begin{bmatrix} p_1(t) \\ p_2(t) - \alpha(1 + d\cos p_1(t))\sin t \end{bmatrix}. \tag{29}$$

Note that c_1 and c_2 are replaced by p_1 and p_2, respectively. Therefore, differentiating (29) with respect to time, i.e., applying (15) to (26), yields (30) shown at the bottom of the page. In slow time $\tau = \omega t$, with a new variable $z(\tau) = p(t)$ as defined in (16), the following standard form is obtained in (31) at the bottom of the page, where $\varepsilon = 1/\omega$.

Finally, by applying the definition of averaging, (18), the following averaged system is obtained:

$$\begin{aligned} \dot{y}_1(t) =& \varepsilon y_2(t), \quad y_1(0) = x_{10} \\ \dot{y}_2(t) =& \varepsilon \frac{d^2\alpha^2}{4} \sin 2y_1(t), \quad y_2(0) = x_{20}. \end{aligned} \tag{32}$$

The control system design in Section III-B is now totally based upon (32) instead of (26). It is noted that the initial conditions of the averaged system does not have to be, in general, the same as those of the original system. It is also noted that a sufficiently small ε can always be obtained since ε was defined by $1/\omega$.

B. Control Strategies for a Free Joint

Fig. 2(a) shows the trajectories of transformed system (30), with $\alpha = 0.5$ and $\omega = 4\pi$ rad/s, departing from various initial conditions in its phase plane. It is noted that two equilibrium points $(\pm\pi/2, 0)$ are centers. It is also observed that fast fluctuating signals are added on top of slow varying signals. Fig. 2(b) shows the phase portrait of averaged system (32) using the same initial conditions as Fig. 2(a). Comparing Fig. 2(a) and (b), it is observed that the slow varying signals in the behavior of (30) is well described by that of (32). Fig. 3 shows the trajectories of the averaged system for various αs. It is observed that by increasing α, the reachable set expands in the vertical direction but the trajectory comes back to its original initial position for all αs. In this paper, an amplitude modulation technique is utilized for reaching an arbitrary point in the state space.

In deriving an averaged system like (32), i.e., in applying (18) to (31), the size of input frequency ω has not been discussed yet. Because the averaging is performed for a period, the input frequency does not matter as far as the final form of averaged system is concerned. But, if the input frequency is too low, the resulted averaged system may not capture the original dynamics well. Fig. 4 shows the discrepancy between the two systems when the input frequency is not fast enough. The trajectory in the left half-plane was not captured by the averaged system. However, the averaging theory assures that for all frequencies above some frequency, i.e., $\forall\ \omega \geq \omega_0$, the averaged system can describe the dynamics of the original system well. Also, by increasing ω, the amplitude of $\theta_1(t)$, as can be seen from (24),

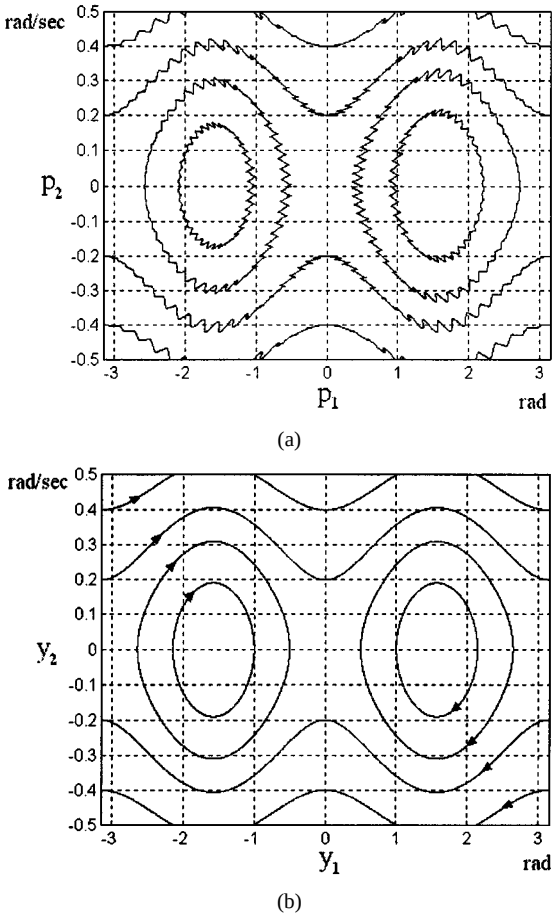

Fig. 2. Comparison of the trajectories of (30) and (32) ($\alpha = 0.5$, $\omega = 4$ rad/s). (a) Trajectories of transformed system (30). (b) Phase portrait of averaged system (32).

$$\begin{aligned} \dot{p}(t) &= \left[\frac{\partial h(\omega t, p(t))}{\partial p}\right]^{-1} X_0\left(h(\omega t, p(t)), \omega t, \frac{1}{\omega}\right) \\ &= \begin{bmatrix} 1 & 0 \\ -\alpha d \sin\omega t \sin p_1(t) & 1 \end{bmatrix} \begin{bmatrix} p_2(t) - \alpha\sin\omega t - \alpha d \sin\omega t \cos p_1(t) \\ -\alpha^2 d \sin p_1(t) \sin^2 \omega t \end{bmatrix} \\ &= \begin{bmatrix} p_2(t) - \alpha\sin\omega t - \alpha d \sin\omega t \cos p_1(t) \\ -\alpha d p_2(t) \sin\omega t \sin p_1(t) + \alpha^2 d^2 \sin^2\omega t \sin p_1(t) \cos p_1(t) \end{bmatrix}. \end{aligned} \tag{30}$$

$$z'(\tau) = \varepsilon \begin{bmatrix} z_2(\tau) - \alpha\sin\tau - \alpha d \sin\tau \cos z_1(\tau) \\ -\alpha d z_2(\tau) \sin\tau \sin z_1(\tau) + \alpha^2 d^2 \sin^2\tau \sin z_1(\tau) \cos z_1(\tau) \end{bmatrix}, \begin{bmatrix} z_1(0) \\ z_2(0) \end{bmatrix} = \begin{bmatrix} x_{10} \\ x_{20} \end{bmatrix} \tag{31}$$

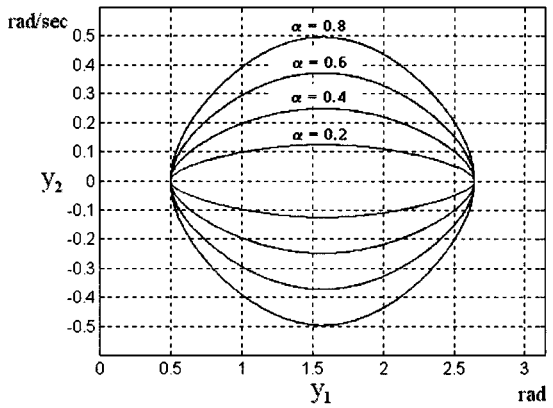

Fig. 3. Trajectory variations of averaged system (32) with various α's ($\omega = 4\pi$ rad/s).

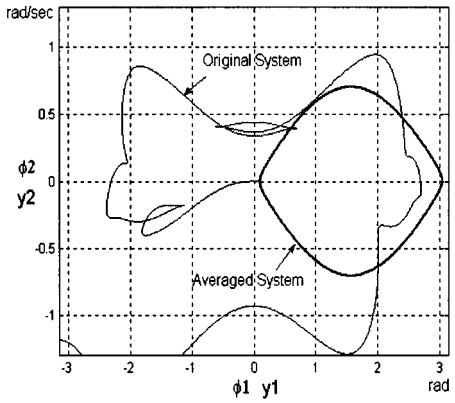

Fig. 4. A discrepancy between two trajectories when the input frequency is not fast enough ($\alpha = 1, \omega = 2$ rad/s).

gets smaller and the Poincare map becomes dense. Therefore, more precise movement can be achieved by increasing ω.

Now, the question is what is the lowest frequency such that beyond that frequency all averaged systems capture the dynamics of the original system well. The answer to the 2R manipulator can be retrieved from (26). Because what we want is that the slow dynamics dominates the fast dynamics, the second term can be set to dominate the first term for selecting sufficiently large ω. Therefore, the following relation can be deduced:

$$\omega\alpha\cos\omega t(1 + d\cos x_1) \gg d\alpha^2 \sin x_1 \sin^2 \omega t.$$

Approximating the above equation, the following lower bound is suggested:

$$\omega_0 \gg K_0 d\alpha$$

where K_0 is a design parameter, which is normally chosen to be bigger than ten from experience.

Let (y_1, y_2) be the present state and (y_{1d}, y_{2d}) be the desired state. The integration of (32) from (y_1, y_2) to (y_{1d}, y_{2d}) yields the following relationship:

$$\frac{d^2\alpha^2}{2}\cos^2 y_1 + y_2^2 = \frac{d^2\alpha^2}{2}\cos^2 y_{1d} + y_{2d}^2. \qquad (33)$$

Observing Fig. 2(b), hovering trajectories are defined as those trajectories in oval form. Therefore, once the initial and target

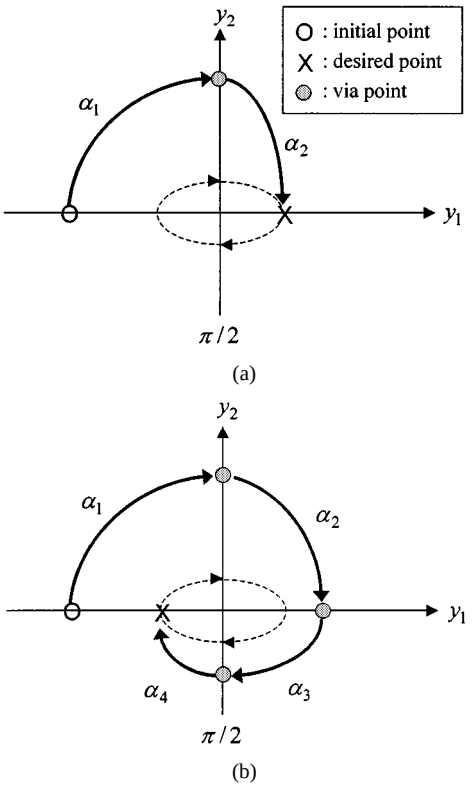

Fig. 5. Two basic steering strategies depending on initial and target positions. (a) When the target distance is greater than $\pi/2$. (b) When the target distance is less than $\pi/2$.

positions are given inside the hovering region, α is uniquely determined by (33). Therefore, the amplitude of a vibration that steers from (y_1, y_2) to (y_{1d}, y_{2d}) is calculated as follows:

$$\alpha = \sqrt{\frac{2\,(y_2^2 - y_{2d}^2)}{d^2\,(\cos^2 y_{1d} - \cos^2 y_1)}}. \qquad (34)$$

Now, an insightful analysis of Figs. 2 and 3 suggests two basic steering strategies that depend on initial and target positions. If the target distance, i.e., $\theta_{2d} - \theta_2$, is more than $\pi/2$ rad, then Fig. 5(a) is suggested. If the target distance is within $\pi/2$ rad, then Fig. 5(b) is suggested. Based upon these two strategies, four control patterns for steering a free joint are sketched in Fig. 6. For example, consider the steering problem from an initial state $(0.5, 0)$ to a desired state $(\pi/4, 0)$, which corresponds to the case of Fig. 6(a). An initial vibration with frequency ω and amplitude α_1 is applied to the active joint θ_1. When θ_2 reaches $\pi/2$, i.e., y_1 becomes $\pi/2$, the amplitude of the vibration is switched from α_1 to $\alpha_{\max}$ for the purpose of reducing traveling time to the target state. If θ_2 begins to decrease, which corresponds to the point that the averaged trajectory crosses the horizontal axis, the amplitude is switched again to α_3 which is supposed to be smaller than α_1. Finally, when θ_2 becomes $\pi/2$ for the second time, the amplitudes are continuously modulated, according to law (34), in each oscillation. The quarter in which amplitudes are modulated in each oscillation is called a cruising quarter. All above observations are summarized in Pattern #1 below. Four different control patterns for various initial and target states are outlined below and their applications are tabulated in Table I.

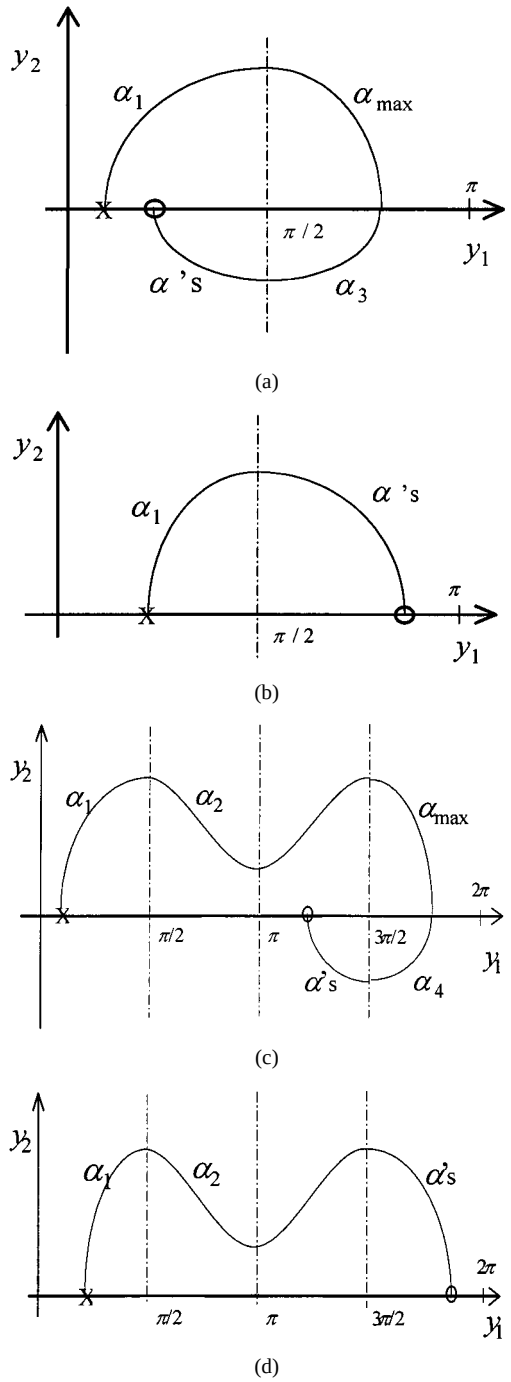

Fig. 6. Four control patterns for a free joint (x: Initial state, O: Target state).

TABLE I
CONTROL PATTERNS BASED UPON INITIAL AND DESIRED POSITIONS

$\theta_2(0)$ \ θ_{2d}	$\left[0, \frac{\pi}{2}\right)$	$\left[\frac{\pi}{2}, \pi\right)$	$\left[\pi, \frac{3\pi}{2}\right)$	$\left[\frac{3\pi}{2}, 2\pi\right)$
$\left[0, \frac{\pi}{2}\right)$	#1	#2	#3	#4
$\left[\frac{\pi}{2}, \pi\right)$	#2′	#1′	#4′	#3′
$\left[\pi, \frac{3\pi}{2}\right)$	#3	#4	#1	#2
$\left[\frac{3\pi}{2}, 2\pi\right)$	#4′	#3′	#2′	#1′

1) ′denotes the reversed patterns in which initial and desired positions are reversed.

2) $\dot{\theta}_2(0) = \dot{\theta}_{2d} = 0$ are assumed.

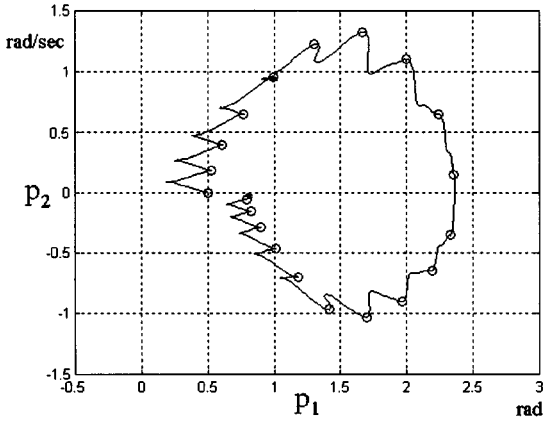

Fig. 7. Simulation of the steering problem from initial angle $\theta_2 = 0.5$ rad to target angle $\theta_2 = \pi/4$ rad following pattern #1 ($\alpha_1 = 1.3$, $\alpha_{\max} = 1.67$, $\alpha_3 = 1.3$, $\omega_1 = 6\pi$, $\omega_2 = 30\pi$).

Pattern #1

Step 1) Set the initial amplitude and frequency at $\alpha = \alpha_1$ and $\omega = \omega_1$, respectively. Fig. 7 shows the trajectories of the second joint from $\left(\theta_1, \dot{\theta}_2\right) = (0.5, 0)$ to $(\pi/4, 0)$ by following Pattern #1. Fig. 7 is a computer-simulated result. The small circles appearing at each period indicate the Poincare map. The initial amplitude and frequency are $\alpha = 1.3$ and $\omega = 6\pi$.

Step 2) If $\theta_2(t)$ becomes $\pi/2$, change α to $\alpha_{\max}$. In Fig. 7, $\alpha_{\max} = 1.67$.

Step 3) If $\theta_2(t)$ gets smaller than its previous value, change α to α_3, where $\alpha_3 \leq \alpha_1$. In Fig. 7, $\alpha_3 = 1.3$.

Step 4) If $\theta_2(t)$ passes $\pi/2$ for the second time, then vary α sequentially in each oscillation according to (34) (the cruising quarter).

Step 5) Finally, if $|\theta_2(t) - \theta_{2d}| < \delta$ where δ is an error bound, switch ω to a higher frequency ω_2. In Fig. 7, $\omega_2 = 30\pi$.

Pattern #2

Step 1) Set initial values: $\alpha = \alpha_1$ and $\omega = \omega_1$.

Step 2) If $\theta_2(t)$ becomes $\pi/2$, then change α sequentially in each oscillation according to (34) (the cruising quarter).

Step 3) Finally, if $|\theta_2(t) - \theta_{2d}| < \delta$, then switch ω to a higher frequency ω_2.

Pattern #3

Step 1) Set initial values: $\alpha = \alpha_1$ and $\omega = \omega_1$.

Step 2) If $\theta_2(t)$ becomes $\pi/2$, choose $\alpha_2 > \alpha(\pi, 0) \triangleq \sqrt{(2y_2^2)/(d^2(1 - \cos^2 y_1))}$, where $\alpha(\pi, 0)$ is

the magnitude of vibration whose averaged trajectory passes through $(\pi, 0)$.

Step 3) If $\theta_2(t)$ becomes $3\pi/2$, switch α to $\alpha_{\max}$.

Step 4) If $\theta_2(t)$ becomes less than its previous value, switch α to α_4, where $\alpha_4 \leq \alpha_1$.

Step 5) If $\theta_2(t)$ becomes $3\pi/2$, change α sequentially in each oscillation according to (34) (the cruising quarter).

Step 6) Finally, if $|\theta_2(t) - \theta_{2d}| < \delta$, switch ω to a higher frequency ω_2.

Pattern #4

Step 1 and Step 2 are the same as Pattern #3.

If $\theta_2(t)$ becomes $3\pi/2$, change α sequentially in each oscillation according to (34).

Finally, if $|\theta_2(t) - \theta_{2d}| < \delta$, switch ω to ω_2.

Finally, it is noted that the first link has to be stopped at an exact period of input in order to keep it at its desired position. It is also noted that, once the free link crosses over its target position, it has to go all the way around again, following Pattern #1, since there is no backward movement. This is because the trajectories move only in clockwise direction, as seen in Fig. 2. Therefore, just before getting to the target position, the input frequency has to be increased to yield precise movements. The achievement of a precise landing at the target position is shown during the last stage of the cruising quarter of Fig. 7 and from the tiny oscillations at the last stage of the control input of Figs. 8 and 11.

C. A 2R Planar Manipulator With a Passive Joint

Let the nonconservative friction force existing at the second joint be $-b_v\dot{\theta}_2 - b_C$, where b_v is the viscous friction coefficient in the bearing and b_C is the Coulomb friction. Then, (21a) and (b) can be written as

$$\ddot{\theta}_1 = u \tag{35a}$$

$$\ddot{\theta}_2 = -(1 + d\cos\theta_2)\ddot{\theta}_1 - d\dot{\theta}_1^2 \sin\theta_2 - f_v\dot{\theta}_2 - f_c \tag{35b}$$

where $f_v = b_v/\left(m_2 l_{2c}^2 + I_2\right)$, $f_c = b_C/\left(m_2 l_{2c}^2 + I_2\right)$. In case that the mass and inertia term of the second link are much larger than the Coulomb friction, f_C can be practically neglected. The frictional effects normally stabilize a system. But in our case the frictions hinder the movement of the joint by dragging it to its equilibrium point. Therefore, the control inputs have to be modified to compensate the existing frictions.

Applying vibrations according to law (11), (23) takes the form as

$$\begin{bmatrix}\dot{x}_1 \\ \dot{x}_2\end{bmatrix} = \begin{bmatrix} x_2 \\ -d\alpha^2 \sin x_1 \sin^2\omega t - f_v x_2 - f_C\end{bmatrix} + \omega\begin{bmatrix}0 \\ -\alpha\cos\omega t(1 + d\cos x_1)\end{bmatrix}. \tag{36}$$

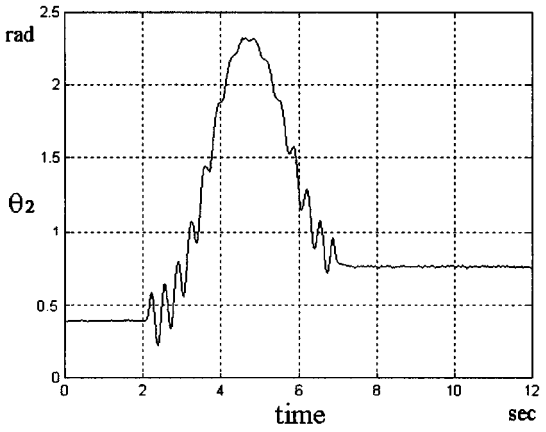

(a)

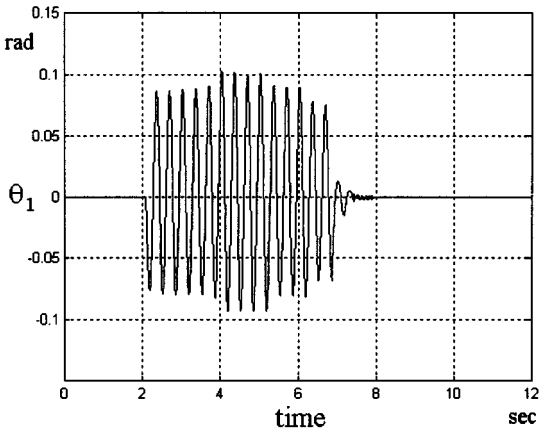

(b)

Fig. 8. Vibrational control of a free joint: $\alpha_1 = 1.3$, $\alpha_{\max} = 1.67$, $\alpha_3 = 1.3$, $\omega_1 = 6\pi$, $\omega_2 = 30\pi$. (a) Position control of a free joint following Pattern #1 (experimental results). (b) Control input used for (a) (experimental results).

Therefore, the generating equation for a passive joint takes the same form as the case of a free joint. The standard form of averaging of (36) now becomes (37) shown at the bottom of the page. Finally, the averaged system is derived as follows:

$$\begin{aligned}\dot{y}_1(t) &= \varepsilon y_2(t),\ dy_1(0) = x_{10} \\ \dot{y}_2(t) &= \varepsilon\left(\frac{d^2\alpha^2}{4}\sin 2y_1(t) - f_v y_2(t) - f_C\right),\ y_2(0) = x_{20}.\end{aligned} \tag{38}$$

D. Control Strategies for a Passive Joint

Fig. 9(a) shows the trajectories of (37) for various initial conditions. It is found that $(\pm\pi/2, 0)$ are two stable foci. Fig. 9(b) shows the phase portrait of (38) for the same initial conditions as Fig. 9(a). As can be seen in Fig. 9(a), the amplitudes decrease due to friction while an individual trajectory goes to an attractor. The overall control strategies for a passive

$$z'(\tau) = \varepsilon\begin{bmatrix} z_2(\tau) - \alpha\sin\tau - \alpha d\sin\tau\cos z_1(\tau) \\ -\alpha d z_2(\tau)\sin\tau\sin z_1(\tau) + \alpha^2 d^2\sin^2\tau\sin z_1(\tau)\cos z_1(\tau) - f_v z_2(\tau) - f_C\end{bmatrix}. \tag{37}$$

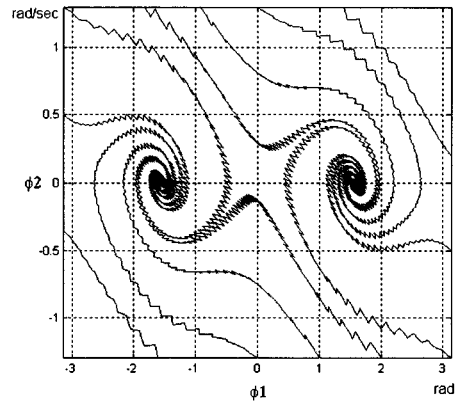

(a)

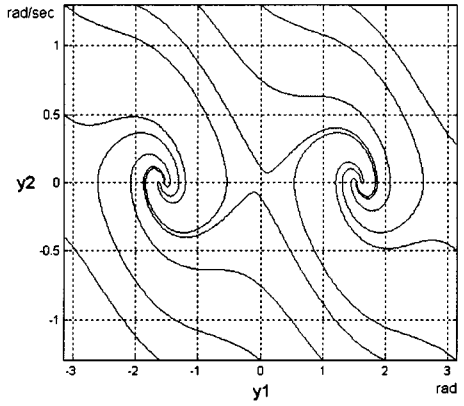

(b)

Fig. 9. Comparison of the trajectories of (37) and (38) ($\alpha = 1$, $\omega = 10\pi$ rad/s). (a) Trajectories of transformed system (37). (b) Phase portrait of averaged system (38).

joint will be the same as the case of a free joint. However, the main obstacle is how to compensate the energy dissipation due to friction. An idea is to increase the amplitudes of vibrations for the purpose of compensating the energy dissipation. Normally it would be difficult to know the exact friction. The exact friction may be identified by some parameter estimation scheme. But, this issue is out of the scope of this paper. In practice, the trend in Fig. 9(a) can be measured using existing sensors. As discussed in Section III-B, α gets smaller near the target position. Therefore, if α is too small, the trajectory may stick to $(\pm\pi/2, 0)$ and becomes unable to move out. Therefore, it is necessary to keep the current trajectory outside an orbit that might be too close to $(\pm/2, 0)$.

Fig. 10(a) shows a trajectory compensation strategy for a passive joint. Let the departure point be $A(y_{1o}, y_{2o})$ and the target point be $B(y_{1f}, y_{2f})$. Let the error between the current point (y_{1r}, y_{2r}) and the target orbit along the vertical direction be e'. Then, e' is calculated as

$$e' = \sqrt{\frac{d^2\alpha_0^2}{2}\left(\cos^2 y_{1o} - \cos^2 y_{1r}\right) + {y_{2o}}^2} - y_{2r}. \qquad (39)$$

Now, a fictitious target point C is inserted on the desired trajectory using B and e'. And, a new input amplitude α_n is calculated using (34). Because the fictitious point C is given by $(y_{1f}, y_{2f} + e')$, α is modified as

$$\alpha_n = \sqrt{\frac{2\left((y_{2f} + e')^2 - y_{2r}^2\right)}{d^2\left(\cos^2 y_{1r} - \cos^2 y_{1f}\right)}}. \qquad (40)$$

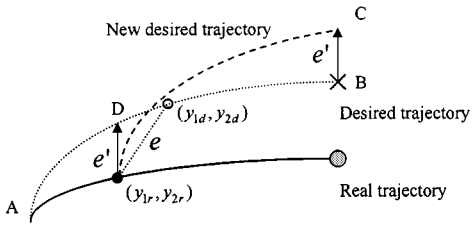

(a)

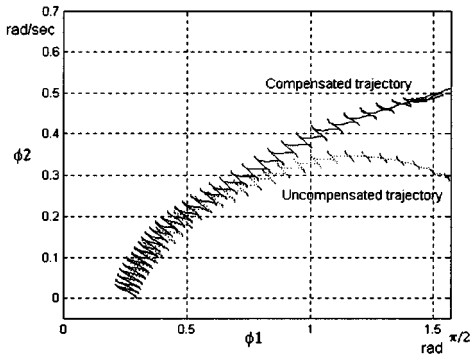

(b)

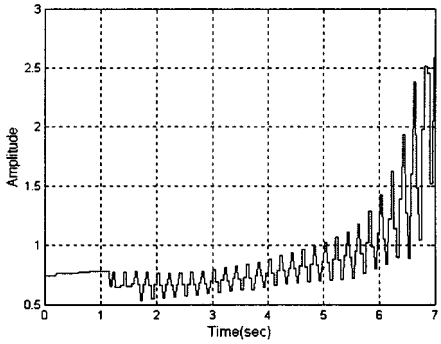

(c)

Fig. 10. A trajectory compensation strategy for a passive joint. (a) A compensation strategy in the presence of friction. (b) Comparison between compensated and uncompensated trajectories: target position $= (\pi/2, 0.5)$. (c) Input amplitudes modulation for (b) starting from an initial value $\alpha_0 = 0.7402$.

Fig. 10(b) demonstrates the steering capability to the target position by a continuous modulation of input amplitudes in the presence of friction, while Fig. 8(c) shows the increasing trend of input amplitudes according to (40).

IV. Experiments

A. Overview

Fig. 1(b) shows the experimental 2R manipulator. The entire setup consists of a 2R mechanism, a data acquisition board, an interface board that includes a servo controller and two signal conditioners, and a PC equipped with a digital signal process card. The manipulator frame is made of aluminum alloy. The

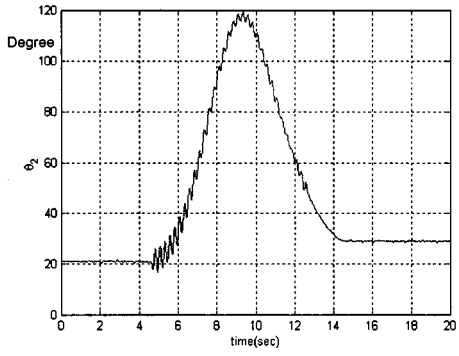

(a)

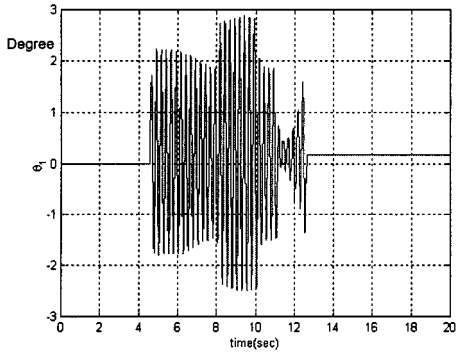

(b)

Fig. 11. Vibrational control of a passive joint (experimental results). (a) Position control of a passive joint (initial position $= 20°$, target position $= 30°$). (b) Motion in time of the first joint: control input for (a).

actuator at the first joint is a high-speed dc coreless motor with a nominal voltage of 12 V and a power consumption of 6 W (Maker: Maxon, Model: 2326). A planetary gear with a gear ratio of 32.1:1 is attached to the head of the motor. A servo controller regulates the input current to the motor, in which the PWM method with a carrier frequency of 20 kHz is used. The rotational angles of both joints are measured by potentiometers. The second link is directly attached to the potentiometer. The damping effect of the potentiometer itself is negligible, but an adjustable slip ring is used for changing friction. The measured signals from the potentiometers are filtered by low-pass filters with a cutoff frequency of 10 Hz before entering the DSP board. The time delay occurring at the low-pass filters is less than 10 μs.

The control algorithm is executed at a DSP board of dSPACE DS1102 with a TI chip TMS320C31. In order to compare simulation and experimental results, the control algorithms are first coded with MATLAB/SIMULINK. Then, after converting them to C codes with Real-Time Workshop, they are downloaded to DS1102 for experiments.

B. Experimental Results

Fig. 8(a) shows the vibrationally controlled motion of a free joint $\theta_2(t)$, in which the initial angle and the target angles were 0.4 rad and $\pi/4$ rad, respectively. Fig. 8(b) shows the motion of the first joint used to invoke the steering force to the second joint, i.e., the control input used for Fig. 8(a). At 2 s, initial vibrations with amplitude 1.3 and frequency 6π were applied. At around 4 s, the amplitude was changed to 1.67, and then 1.3 following Pattern #1. The tiny oscillations appearing after 7 s indicate that the frequency has been increased to $\omega_2 = 30\pi$. Experimental results agree well with simulation results.

In order to increase friction at the second joint, an adjustable slip ring has been used. Fig. 11(a) shows an experimental result of vibrational control of a passive joint for a given initial position at 20° and a target position 30°. Fig. 11(b) shows the input vibrations used for Fig. 11(a). As seen in Fig. 11(b), the input amplitudes have been modulated according to (40).

V. Conclusion

An open loop vibrational control for an underactuated mechanical system has been investigated. To move an unactuated joint, the dynamic coupling occurred due to the oscillatory motion of the actuated joint was utilized. A generating equation for deriving a coordinate transformation was derived from the unactuated joint dynamics. The input amplitudes were determined by analyzing an averaged system representing the unactuated joint dynamics with a periodic input. The averaging method was extended to the system with the derivatives and antiderivatives of vibrations. To demonstrate detailed design steps, a 2R planar manipulator with a free joint and a passive joint was used. In zero gravity space, a manipulator with a failed joint can be controlled in this manner. Considering the fact that the method in this paper can control an uncontrollable system, it will provide a viable tool when the conventional control schemes are not applicable.

References

[1] H. Arai and S. Tachi, "Position control of a manipulator with passive joints using dynamic coupling," *IEEE Trans. Robot. Automat.*, vol. 7, pp. 528–534, 1991.

[2] H. Arai, K. Tani, and S. Tachi, "Dynamic control of a manipulator with passive joints in operational space," *IEEE Trans. Robot. Automat.*, vol. 9, pp. 85–93, 1993.

[3] J. Beillieul and B. Lehman, "Open-loop control using oscillatory inputs," in *The Control Handbook*, W. S. Levine, Ed. Boca Raton, FL: CRC , 1996, vol. II, pp. 967–980.

[4] ——, "Vibrational control of nonlinear systems: Vibrational stabilizability," *IEEE Trans. Automat. Contr.*, vol. 31, pp. 710–716, 1986.

[5] ——, "Vibrational control of nonlinear systems: Vibrational controllability and transient behavior," *IEEE Trans. Automat. Contr.*, vol. 31, pp. 717–724, 1986.

[6] J. Bentsman and K. S. Hong, "Vibrational stabilization of nonlinear parabolic systems with Neumann boundary condition," *IEEE Trans. Automat. Contr.*, vol. 36, pp. 501–507, 1991.

[7] J. Bentsman, K. S. Hong, and J. Fakhfakh, "Vibrational control of nonlinear time lag systems: Vibrational stabilization and transient behavior," *Automatica*, vol. 27, no. 3, pp. 491–500, 1991.

[8] J. Bentsman and K. S. Hong, "Transient behavior analysis of vibrationally controlled nonlinear parabolic systems," *IEEE Trans. Automat. Contr.*, vol. 38, pp. 1603–1607, 1993.

[9] M. Bergerman and Y. Xu, "Optimal control for underactuated manipulators," in *Proc. 1996 IEEE Int. Conf. Robot. Automat.*, Minneapolis, MN, 1996, pp. 3714–3719.

[10] N. N. Bogoliubov and Y. A. Mitropolskii, *Asymptotic Methods in the Theory of Nonlinear Oscillators*. New York: Gordon and Breach, 1961.

[11] S. A. Bortoff, "Approximate feedback linearization using spline functions," *Automatica*, vol. 33, no. 8, pp. 1449–1458, 1997.

[12] A. De Luca, R. Mattone, and G. Oriolo, "Steering a class of redundant mechanisms through end-effector generalized forces," *IEEE Trans. Robot. Automat.*, vol. 14, pp. 329–335, 1998.

[13] J. Guckenheimer and P. Holmes, *Nonlinear Oscillations, Dynamical Systems, and Bifurcations of Vector Fields*. New York: Springer-Verlag, 1983.

[14] K. S. Hong and J. Bentsman, "Stability criterion for linear oscillatory parabolic systems," *ASME J. Dynamic Syst., Measurement, Contr.*, vol. 114, no. 1, pp. 175–178, 1992.

[15] ——, "Application of averaging method for integro-differential equations to model reference adaptive control of parabolic systems," *Automatica*, vol. 30, no. 9, pp. 1415–1419, 1994.

[16] K. S. Hong, K. R. Lee, and K. I. Lee, "Vibrational control of underactuated mechanical systems: Control design through averaging analysis," in *Proc. Amer. Contr. Conf.*, Philadelphia, PA, 1998, pp. 3482–3486.

[17] B. Lehman, J. Bentsman, S. V. Lunel, and E. I. Verriest, "Vibrational control of nonlinear time lag systems with bounded delays: Averaging theory, stabilizability, and transient behavior," *IEEE Trans. Automat. Contr.*, vol. 39, pp. 898–912, 1994.

[18] A. De Luca, R. Mattone, and G. Oriolo, "Stabilization of underactuated robot: Theory and experiments for a planar 2R manipulator," in *Proc. IEEE Int. Conf. Robot. Automat.*, Albuquerque, NM, 1997, pp. 3274–3280.

[19] S. M. Meerkov, "Principle of vibrational control: Theory and applications," *IEEE Trans. Automat. Contr.*, vol. 25, pp. 755–762, 1980.

[20] R. M. Murray, Z. Li, and S. S. Sastry, *A Mathematical Introduction to Robotic Manipulation*. Boca Raton, FL: CRC, 1994.

[21] Y. Nakamura, T. Suzuki, and M. Koinuma, "Nonlinear behavior and control of a nonholonomic free-joint manipulator," *IEEE Trans. Robot. Automat.*, vol. 13, pp. 853–862, 1997.

[22] F. Saito, T. Fukuda, and F. Arai, "Swing and locomotion control for a two-link brachiation robot," *IEEE Contr. Syst. Mag.*, vol. 14, no. 1, pp. 5–12, 1994.

[23] C. Samson, "Control of chained systems application to path following and time-varying point-stabilization of mobile robots," *IEEE Trans. Automat. Contr.*, vol. 40, pp. 64–77, 1995.

[24] J. A. Sanders and F. Verhulst, *Averaging Methods in Nonlinear Dynamical System*. New York: Springer-Verlag, 1990.

[25] S. Sastry and M. Bodson, *Adaptive Control: Stability, Convergence, and Robustness*. Englewood Cliffs, NJ: Prentice-Hall, 1989.

[26] W. Singhose, N. Singer, and W. Seering, "Time-optimal negative input shapers," *ASME J. Dynamic Syst., Measurement, Contr.*, vol. 119, no. 2, pp. 198–205, 1997.

[27] M. W. Spong, R. Marino, S. Peresada, and D. G. Taylor, "Feedback linearizing control of switched reluctance motors," *IEEE Trans. Automat. Contr.*, vol. 32, pp. 371–379, 1987.

[28] M. W. Spong, "The swing up control problem for the acrobot," *IEEE Contr. Syst. Mag.*, vol. 15, no. 1, pp. 49–55, 1995.

[29] T. Suzuki and Y. Nakamura, "Nonlinear control of a nonholonomic free joint manipulator with the averaging method," in *Proc. 35th IEEE Conf. Decision Contr.*, Kobe, Japan, 1996, pp. 1694–1699.

[30] ——, "Control of manipulators with free-joints via the averaging method," in *Proc. IEEE Int. Conf. Robot. Automat.*, 1997, pp. 2998–3005.

[31] T. Suzuki, W. Miyoshi, and Y. Nakamura, "Control of 2R underactuated manipulator with friction," in *Proc. 37th IEEE Conf. Decision Contr.*, Tampa, FL, 1998, pp. 2007–2012.